Kinetic Properties of Single Sodium Channels in Rat Heart and Rat Brain

G. E. KIRSCH and A. M. BROWN

From the Department of Physiology and Molecular Biophysics, Baylor College of Medicine, Houston, Texas 77030

ABSTRACT Single Na channel currents were compared in ventricular myocytes and cortical neurons of neonatal rats using the gigaseal patch-clamp method to determine whether tissue-specific differences in gating can be detected at the single-channel level. Single-channel currents were recorded in cell-attached and excised membrane patches at test potentials of −70 to −20 mV and at 9–11°C. In both cell-attached and excised patches brain Na channel mean open time progressively increased from <1 ms at −70 mV to ~2 ms at −20 mV. Near threshold, single openings with dispersed latencies were observed. By contrast, in cell-attached patches, heart Na channel mean open time peaked near −50 mV, was three times brain Na channel mean open time, and declined continuously to ~2 ms at −20 mV. Near threshold, openings occurred frequently usually as brief bursts lasting several milliseconds and rarely as prolonged bursts lasting tens of milliseconds. Unlike what occurs in brain tissue where excision did not change gating, in excised heart patches both the frequency of prolonged bursting and the mean open time of single units increased markedly. Brain and cardiac Na channels can therefore be distinguished on the basis of their mean open times and bursting characteristics.

INTRODUCTION

Voltage-dependent Na channels are responsible for generating action potentials in many types of excitable cells. In mammals the voltage-dependent Na channel of nerve, heart, and skeletal muscle differ in their pharmacological properties. Tetrodotoxin (TTX) blocks cardiac Na channels at micromolar concentrations and nerve Na channels at nanomolar concentrations (Narahashi, 1974), conversely, lidocaine blocks cardiac Na channels with 1,000 times greater potency than it blocks neuronal Na channels (Bean et al., 1983). A third agent, μ-contoxin, blocks skeletal muscle Na channels but has no effect on neuronal or cardiac Na channels (Cruz et al., 1985).

Tissue-specific differences in gating kinetics have been reported also. Inactivation of Na current in cardiac myocytes consists of a fast, and one or more slow phases (Brown et al., 1981; Kunze et al., 1985; Follmer et al., 1987). The slow components may contribute to the plateau of the cardiac action potential since Na channel blockers such as TTX and lidocaine shorten the action potential (Dudel et al., 1967;

Address reprint requests to Dr. G. E. Kirsch, Department of Physiology and Molecular Biophysics, Baylor College of Medicine, One Baylor Plaza, Houston, TX 77030.

J. GEN. PHYSIOL. © The Rockefeller University Press · 0022-1295/89/01/0085/15 $2.00
Volume 93 January 1989 85–99

Davis and Temte, 1969). Slow components are much less prominent in nerve (Chiu, 1977).

In this report we show that under identical recording conditions, there are large differences in single Na channel currents from brain and heart. At threshold potentials single-channel currents in cell-attached heart patches were characterized by a mixture of isolated brief openings and long bursts, which upon patch excision became predominantly long bursts. In contrast, neuronal single-channel currents showed single openings with dispersed first latencies and the pattern was the same in both cell-attached and excised patch conditions.

A preliminary report of these results has been published (Kirsch and Brown, 1988).

METHODS

Solutions and Drugs

Experiments were performed in a chamber that was placed on a temperature-controlled microscope stage and filled with 0.6 ml extra- or intracellular solution, depending on the recording mode. Extracellular solution for patch recording consisted of (in millimolar): 137 NaCl, 5.4 KCl, 1.0 $MgCl_2$, 1.8 $CaCl_2$, 10 glucose, 5 HEPES, pH 7.4. Depolarizing bath solution used in cell-attached experiments in heart contained either KCl or KF as a replacement for NaCl, and Mg^{2+} as a replacement for Ca^{2+}. The internal solution for outside-out excised patch recording consisted of (in millimolar): 120 CsF, 11 EGTA, 2 $MgCl_2$, 10 HEPES, pH 7.4. All experiments were performed at 9–11°C.

Cell Culture

Primary cardiac cell cultures were prepared from hearts of neonatal rats (1–3 d old) as described previously (Yatani and Brown, 1985). Briefly, hearts were removed under sterile conditions, and the ventricles were cut into pieces and incubated at 37°C for 5 min in Ca-free Hanks solution containing 0.5% trypsin (T-0134; Sigma Chemical Co., St. Louis, MO). The supernatant was removed and the pelleted cells were added to Dulbecco's modified Eagle's medium with 10% fetal calf serum (DMEM-10 FCS) culture medium, to stop enzyme action. Resuspended cells were seeded in glass coverslips and incubated in culture medium at 37°C in a 5% CO_2-95% O_2 atmosphere. Recording was performed on days 1–2 after seeding.

Neuronal cell cultures were prepared from the cortex of neonatal (1–3 d old) rat brains that were dissociated into single cells by passing tissue suspensions through 0.04-mm nylon mesh filters. Cells were pelleted from the filtrate, resuspended, and plated on poly-D-lysine coated coverslips. After a 24-h incubation at 37°C in DMEM-10 FCS, the cells were placed in a serum-free defined medium selective for neuronal growth (DMEM supplemented with insulin, transferrin, progesterone, putrescine, and sodium selenite). Recording was performed 7–14 d after seeding. We selected neurons with ellipsoidal somota and bipolar cell processes. These cells had a lower channel density than pyramidal cells, hence, were more suitable for single-channel recording.

Electrophysiological Recording

Patch-clamp recording was performed using techniques described previously (Hamill et al., 1981; Lux and Brown, 1984). Single-channel Na currents were recorded from membrane patches using Sylgard-coated micropipette (Corning 7052 glass; Corning Glass Works, Corning, NY) with resistances of 10–15 MΩ connected to a commercial patch-clamp amplifier

(EPC-7; List Co., Darmstadt, FRG). Currents evoked by 140-ms depolarizing test pulses were stored on videocassette tape (PCM-1; Medical Systems Corp., Great Neck, NY) at a bandwidth of 16 kHz. The data were later digitized by a PDP-11/73 computer (Digital Equipment Corp., Marlboro, MA) with 12-bit resolution at a sample rate of 10 kHz after low-pass filtering at 3.15 kHz (−3 dB) using a four-pole Bessel filter (Ithaco Inc., Ithaca, NY). Digitized records were corrected off-line for linear leakage and capacitative currents by subtracting the average of records lacking single-channel activity, then they were digitally filtered using a zero-phase four-pole low-pass Bessel filter at 1.4 kHz prior to level detection. Transitions between closed and open levels were determined using an interactive threshold detection program in which the opening threshold was set at half-maximum amplitude of single-unit opening. Computer-detected openings were confirmed by visual observation and used to generate idealized records from which histograms of amplitude, waiting, closed-, and open-time distributions were constructed. Amplitude histograms were fit by Gaussian functions using a χ^2 nonlinear regression routine. Single units of <0.4-ms duration were excluded from the histogram to avoid truncation errors introduced by the limited frequency response of the recording system. Waiting-time distributions were obtained by determining the latency between the beginning of each test pulse and the first channel event detected in the record. The distributions were corrected for the number of channels in a patch and estimated from channel overlap at potentials of −20 to −10 mV by the method of Patlak and Horn (1982). Open-time distributions were constructed from data sets in which events consisting of overlapping openings of two or more channels were excluded. Prepulse potentials (100-ms duration) were adjusted to ensure that the fraction of such events was <15% of the total events at a given test potential to minimize the bias introduced by excluding overlaps. The sum of idealized records at a given test potential was used to reconstruct macroscopic currents. Mean open times, waiting times, and macroscopic current decay-time constants were calculated by fitting the data to the sum of exponential decay functions using a maximum likelihood estimate. The accuracy of fitting biexponential models in preference to monoexponentials was evaluated by a ratio of variance (F test). Where appropriate, data are expressed as mean ±SE. Significance of differences between means was evaluated using a two-tailed Student's t test ($P = 0.05$).

RESULTS

Neurons of neonate rat cortex contain a high density of Na channels such that outside-out membrane patches sometimes contained more than 20 channels. In such patches "quasimacroscopic" Na currents could be recorded and these records sometimes showed evidence of more than one type of inward current channel as shown in Fig. 1. In Fig. 1 *A* four sample records are shown at low gain. Each record was evoked by a test potential of −40 mV from a holding potential of −100 mV; the records are uncorrected for leakage or capacitative currents since no null traces were recorded under these conditions. Each trace shows a large inward transient current, which, when averaged over the entire run of 57 records (Fig. 1 *D*) gave a mean peak current of 18 pA. As shown in Fig. 1 *E*, 3 μM TTX reduced the peak amplitude by 96%; therefore, this current arises predominantly from Na channels, the single-channel openings of which cannot be distinguished owing to the large number of channels in the patch. The inactivation phase of the summed currents in the absence of TTX (Fig. 1 *G*, lower trace) could be accurately fit to a biexponential decay with time constants of 3.7 and 12.4 ms, the fast phase representing about 84% of the decay. In the presence of TTX the fast phase of inactivation was elimi-

nated and the decay phase of the residual TTX-resistant current could be fit to a monoexponential function with a time constant of 10.2 ms. This slowly inactivating current may belong to the TTX-resistant Na currents previously reported in rat neurons by Kostyuk et al. (1981). Such currents constituted a very minor component and were only seen in patches containing a large number of channels.

A third type of inward current is also illustrated in Fig. 1 *B*, where in the presence of TTX, records obtained at higher gain reveal the presence of brief, low amplitude channel openings throughout the trace. Such openings are responsible for the increased baseline noise during the pulse as compared with the tail portion of the

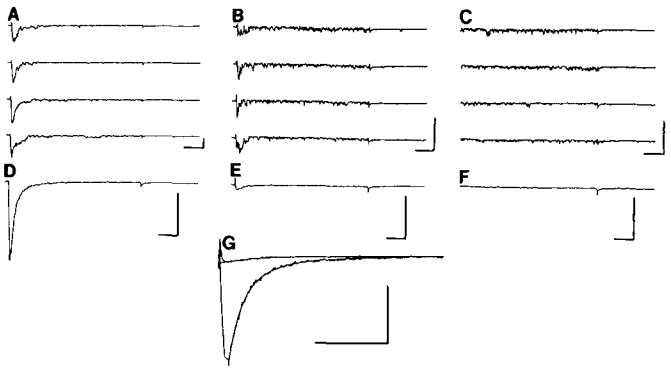

FIGURE 1. Inward currents recorded in an outside-out patch from a rat cortical neuron. Inward currents are downward deflections. *A* and *B* show sample records evoked by test pulse potential of −40 mV, holding potential −100 mV, in the presence (*B*) and absence (*A*) of 3 μM TTX. In *C*, the test pulse was preceded by a 100-ms prepulse to −40 mV to inactivate residual TTX-resistant Na channels. *D* and *E* show mean current obtained by averaging 50–60 records from experiments in *A–C*. In *G*, the records from *D* and *E* are shown on an expanded time scale and with exponential curve-fitting (smooth line) of the decay phase. The time constants (and weighting factors) for the lower trace (control) were 3.7 (0.84) and 12.4 (0.16) ms. The time constant obtained from the upper trace (TTX) was 10.2 ms. Records were filtered at 3.15 kHz (−3 dB), digitized at 10 kHz, and digitally filtered at 1.4 kHz. No off-line correction was made for leakage or capacitative currents. Residual capacity transients mark the beginning and end of the test pulse. The vertical and horizontal calibration bars represent 10 pA and 20 ms, respectively. Note that the gain in *A* is one-third that of *B* and *C*, and that the time-base of *G* is expanded relative to *A–F*. Temperature, 10.0°C.

record. In other experiments (not shown) we determined the single-channel amplitude of the noninactivating component to be roughly one-half that of the TTX-sensitive Na channel. The channels responsible are apparently voltage sensitive (since they are absent at the resting potential in Fig. 1, *A–C*), TTX insensitive, and resistant to inactivation. In Fig. 1 *C* a depolarizing prepulse eliminated the inactivation-sensitive TTX-resistant channels leaving only the third component of inward current. As shown in Fig. 1 *F* this component adds little to the summed current, however, single-channel records of TTX-sensitive Na channels can be contaminated by bursts of openings originating from this noninactivating channel. In the following we describe the properties of the major TTX-sensitive Na channel in these neu-

rons. Patches that contained TTX-resistant or noninactivating channels were not included in the analysis.

Open times and frequency of reopening are the most striking differences between brain and cardiac single-channel Na currents. Fig. 2 shows single-channel currents obtained in outside-out patches from a ventricular myocyte (*A–C*) and a cortical neuron (*D* and *E*) recorded under identical conditions. Each patch contained four channels as estimated from the maximum number of simultaneous openings at depolarized test potentials. As shown in Fig. 2 *A* at a test potential of −60 mV, heart channels tend to open in long-lasting bursts consisting of repetitive long openings

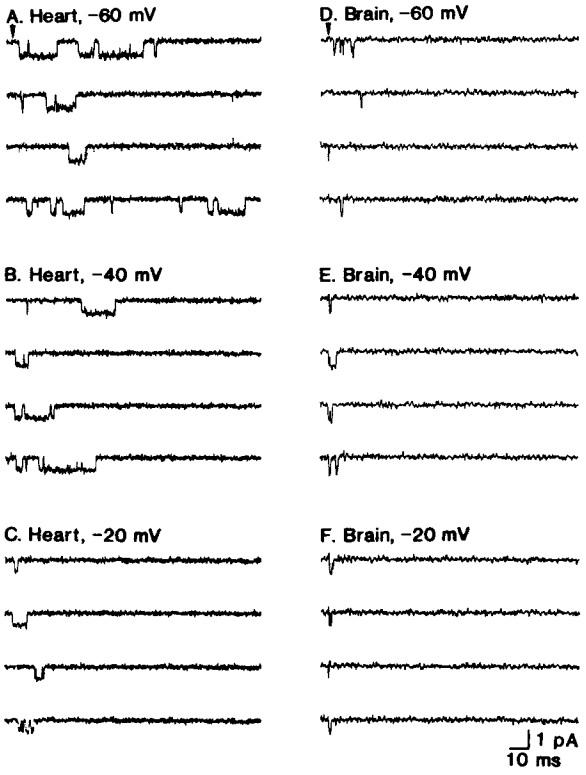

FIGURE 2. Single Na channel currents in outside-out patches from a ventricular myocyte (*A–C*) and a cortical neuron (*D–F*). Each panel shows records evoked by 140-ms test pulses (onset marked by arrow) to the potential indicated from a holding potential of −100 mV. In *A–C* each test pulse was preceded by a 100-ms prepulse to −120 mV. End of trace coincides with end of test pulse. Pulses were delivered at 1 Hz. Channel openings are indicated by downward deflections. Records were filtered at 3.15 kHz (−3 dB), digitized at 10 kHz, and digitally filtered at 1.4 kHz. Capacitative and leakage currents were minimized by using Sylgard-coated electrodes and electronic compensation. Final correction was made by digital subtraction of records containing no activity. Temperatures were 10.9°C (*A–C*) and 10.1°C (*D–F*).

interrupted by very brief closures. In contrast, brain channels (Fig. 2 *D*) open briefly and rarely reopen. At a test potential of −20 mV (Fig. 2, *C* and *F*), reopening was infrequent in both heart and brain, however, both the duration of individual openings and the latency to first opening (waiting time) were longer in heart than in brain channels. The kinetic differences were not associated with differences in conductance. Mean single-channel conductances were 9.2 and 8.7 pS in heart and brain, respectively.

Averaged single-channel currents (Fig. 3) confirm that both quantitative and qualitative differences in the time course of membrane Na conductance result from the

observed differences in single-channel currents. The activation phase of the averaged currents was more than two times faster in brain than in heart (note the faster time base of records *D–F* compared with *A–C*). As shown below, the slower activation kinetics in heart are reflected in the single-channel waiting-time distribution. Furthermore, in neurons (Fig. 3, *D–F*) the time course of macroscopic inactivation, represented by the decay phase of the summed single-channel records, was accurately fit by a monoexponential decay with time constants ranging from 8 to 1 ms at test potentials of −60 to −20 mV, respectively. Inactivation in heart cells (Fig. 3, *A–C*), by contrast, was accurately fit by the sum of two exponentials such that the overall decay time decreased with depolarization, but at all potentials were much longer than in neurons. Thus, in heart a significant fraction of peak current remains even after 40 ms of depolarization to −60 mV (Fig. 3 *A*).

The slow components of macroscopic current in heart must arise from channels

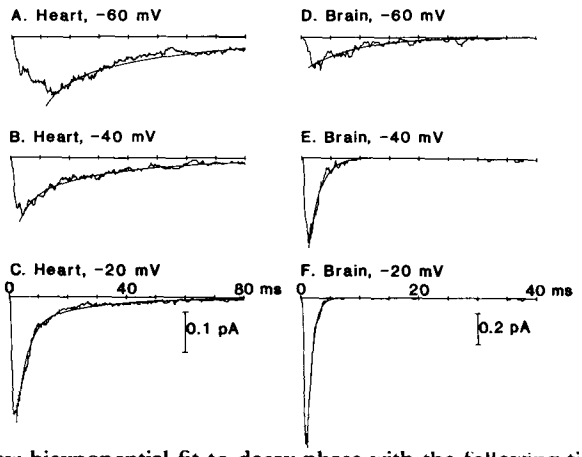

FIGURE 3. Reconstruction of macroscopic currents from single-channel records in a ventricular myocyte (*A–C*) and a cortical neuron (*D–F*). Same experiments as Fig. 2. In each panel single-channel records obtained at the indicated potentials were summed and the average current was calculated. Calibrations in *C* and *F* apply to panels *A–C* and *D–F*, respectively. Note that the time base of *A–C* is slower than *D–F*. Smooth curves in *A–C* show biexponential fit to decay phase with the following time constants (and weighting factors): (*A*) 6.5 ms (0.7) and 48.8 ms (0.3), (*B*) 4.7 ms (0.6) and 33.9 ms (0.4), (*C*) 3.4 ms (0.9) and 23.5 ms (0.1). Smooth curves in *D–F* show monoexponential fits with time constants: (*D*) 8.3 ms, (*E*) 1.9 ms, (*F*) 0.9 ms.

that (*a*) opened at a much earlier time and remained open for a variable interval during the decay phase, (*b*) open only briefly with waiting times dispersed throughout the decay phase, or (*c*) repetitively open and close during the decay phase. In the following section we provide evidence for the latter explanation. Neuronal channels, in contrast, follow a kinetic pattern more closely resembling (*b*).

Kinetic analysis of single-channel records is presented in Fig. 4. The open-time histogram for heart channels at a test potential of −60 mV (Fig. 4 *A*) was accurately fit by a monoexponential decay with time constants of 5.5 ms compared with 0.7 ms in brain channels (Fig. 4 *D*). At more depolarized test potentials (not shown) mean open time in heart channels progressively decreased, reaching 2.6 ms at −20 mV. By contrast, open time in brain was relatively independent of test potential; mean open time increased to 0.9 ms at −20 mV. Thus, an important distinction between the two channel types is that heart channels stay open for a much longer time than brain channels, which is at least in part due to longer mean open times; the differ-

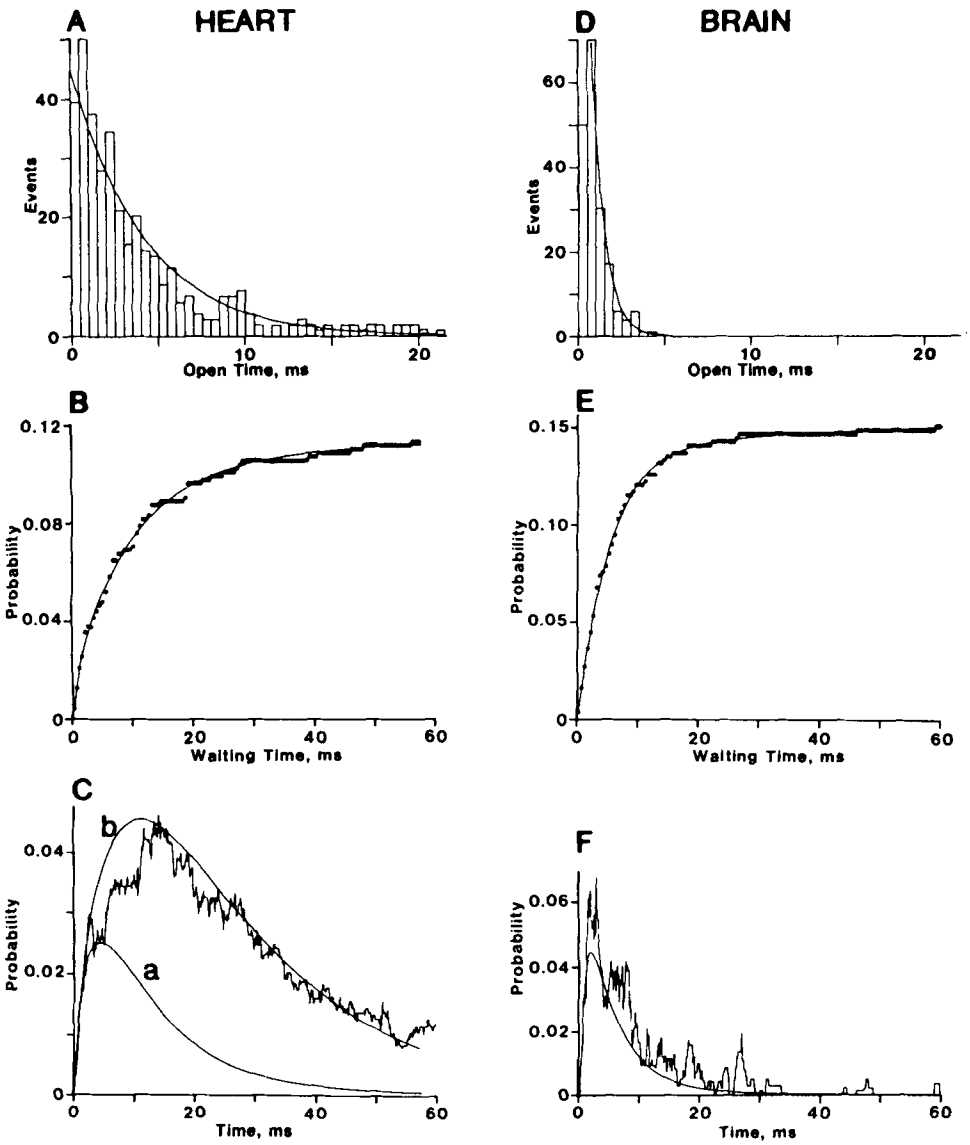

FIGURE 4. Analysis of open and waiting times at −60 mV in a ventricular myocyte (*A–C*) and a cortical neuron (*D–F*). Same experiments as in Fig. 2. Open-time frequency histograms in *A* and *D* were fit to monoexponential distributions using a Marquardt algorithm and a maximum likelihood estimator. Time constants were 4.2 and 0.7 ms, respectively, in *A* and *D*. Frequency distributions of waiting times (*B* and *E*), plotted as a cumulative histogram, were corrected for four channels by the method of Patlak and Horn (1982). Smooth curves are biexponential fits with the following time constants (and weighting factors): (*B*) 6.9 ms (0.51) and 16.7 ms (0.49), (*E*) 5.8 ms (0.99) and 82.2 ms (0.1). *C* and *F* compare the convolution of the open- and waiting-time distributions (smooth curve) with the time course of probability of opening (P_o-*t*, noisy trace). Fitted curves rather than histograms were convolved to produce the smooth curves in *C* and *F*. The convolution should accurately predict P_o-*t* when channels open with dispersed latencies but do not reopen, as in the Aldrich-Corey-Stevens kinetic model (1983).

ence was most pronounced at −60 mV where the mean open time of heart channels was sevenfold longer than that of brain channels. Furthermore, mean heart open time appears to have a different voltage sensitivity: open time decreases with depolarization whereas brain open time increased slightly.

These results rule out explanation (*a*) above, which requires that the macroscopic decay time constant approximate the mean open time. In both tissues, the two parameters became roughly equal at test potentials greater than −30 mV; at more negative potentials either reopening or dispersed latencies are required to account for macroscopic inactivation.

As shown in Fig. 4, *B* and *D*, cumulative waiting time distributions in both heart (*B*) and brain (*C*) could be described by the sum of two exponentials, in heart, however, roughly one-half the area under the waiting-time curve was accounted for by a slow component with a time constant of 17 ms, whereas the major (0.99) time constant in brain was 6 ms. Similarly, the waiting time at −20 mV (not illustrated) was fourfold longer in heart than in brain. Since the waiting times reflect transition rates from closed to open states it is apparent that these transitions occur much more slowly in heart than in brain.

As a test of the importance of reopening to the time course of the decay phase of macroscopic currents, we performed a convolution of the waiting time with the open-time distributions. If each channel opens only once, convolving the waiting time with the open time should give the time course of the probability of single-channel opening (P_o-t relationship; Aldrich et al., 1983). Fig. 4 illustrates convolutions for data obtained at a test potential of −60 mV in heart (*C*) and brain (*F*). In Fig. 4 *F* the close superposition of the convolution (smooth curve) with the P_o-t relationship (noisy trace) suggests that dispersed waiting times contribute to macroscopic inactivation in agreement with the Aldrich-Corey-Stevens (1983) model, whereas the poor fit in Fig. 4 *C* (curve *a*) shows that heart channels follow a different kinetic scheme. Waiting times in heart channels, although longer than in brain, are still too short to account for the time course of macroscopic inactivation. A better fit, however, was obtained by convolving the waiting time with total open time within bursts (Fig. 4 *C*, curve *b*, burst analysis described below). Our results, in agreement with Kunze et al. (1985) suggest that at potentials of −60 to −40 mV, prolonged bursting is an important kinetic feature of heart Na channels.

The reopening behavior of heart channels was analyzed by identifying bursts that originated from single channels. As shown in Fig. 5 *A* the frequency distribution of closed times was accurately described by two well-resolved time constants, the shortest of which was assumed to arise from closed-time intervals within bursts. Using the criterion of Colquhoun and Sakmann (1985) we estimated that a critical closed duration of 1.7 ms would adequately distinguish single-channel bursts. Since the reliability of this estimate decreases with the number of channels in the patch (four channels in Fig. 5) we performed similar analysis on another patch that contained only two channels, in which case the critical duration was 1.1 ms. As shown in Fig. 5 *B*, the burst duration frequency of the four-channel patch was distributed equally between short (3 ms) and long (17 ms) bursts. For the long bursts, the average number of openings per burst was 3.5. In the two-channel patch (not illustrated) burst duration time constants (and weighting factors) of 2.3 (0.6) and 12.2 (0.4) ms were obtained. Long bursts contained on average three openings.

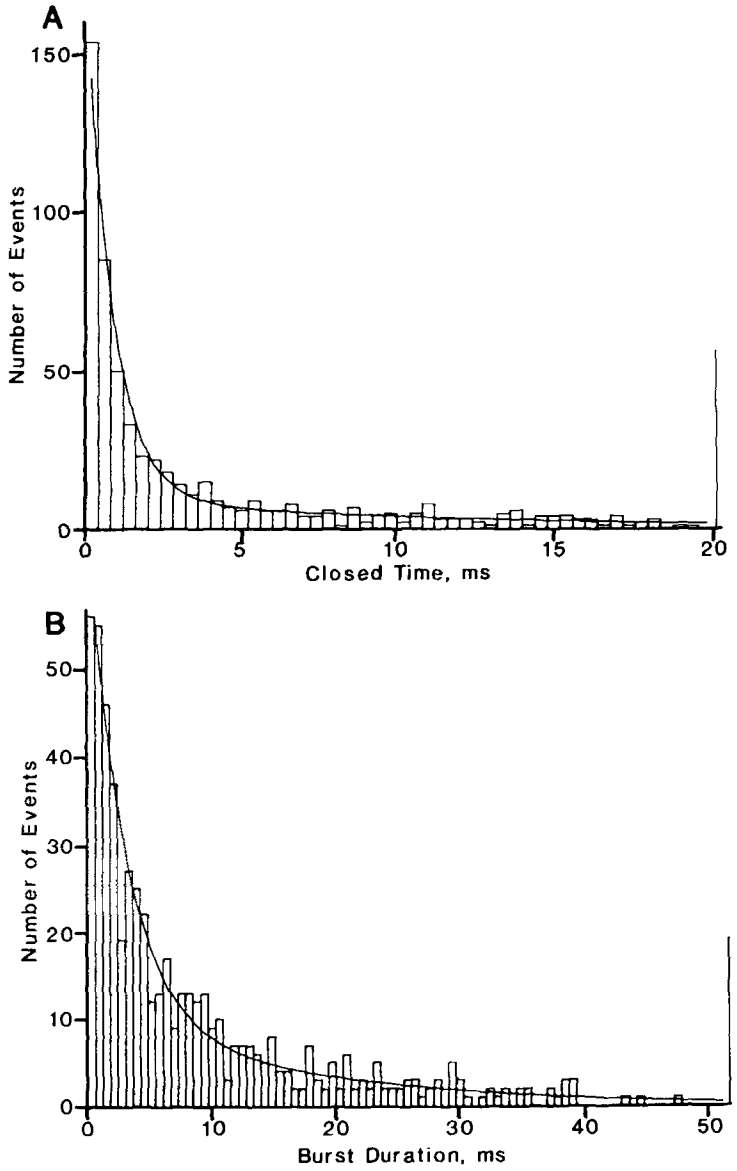

FIGURE 5. Analysis of bursts in an outside-out patch from a ventricular myocyte at a test potential of −60 mV. Same experiment as in Fig. 2. Frequency distribution of closed times (*A*) was fit to a biexponential decay with time constants (and weighting factors) 0.8 (0.42) and 13.9 (0.58) ms. The vertical line at 20 ms represents the number of closed time intervals that are >20 ms (56) and off scale. Events containing overlapping openings of multiple channels were excluded (10% of total number of events). From the two closed-time constants and the assumption that the brief closed time arises from single-channel bursts, 1.7 ms was calculated as the maximum closed time within a burst (Colquhoun and Sakmann, 1985). Frequency distribution of burst durations is shown in *B*. The smooth curve is a biexponential distribution with time constants (and weighting factors) 3.0 ms (0.49) and 17.1 ms (0.51). Burst durations longer than 50 ms (vertical bar at right, 19 events) are off scale.

Fig. 6 compares the voltage dependence of the mean open time in heart and brain Na channels. In excised patches (filled symbols) mean open time of heart channels showed a weak voltage dependence of roughly an e-fold decrease/46 mV depolarization in the test potential range −60 to −20 mV, whereas brain channel open time increased slightly in this voltage range. However, when data from cell attached patches (open symbols) from heart and brain were compared, the mean open time at −20 mV was identical and the differences at lower depolarizations were less marked. This change appears to be due almost entirely to differences between the open-time distributions of heart Na channels in excised and cell-attached patches; open-time distribution in neuronal patches was resistant to excision-induced modification.

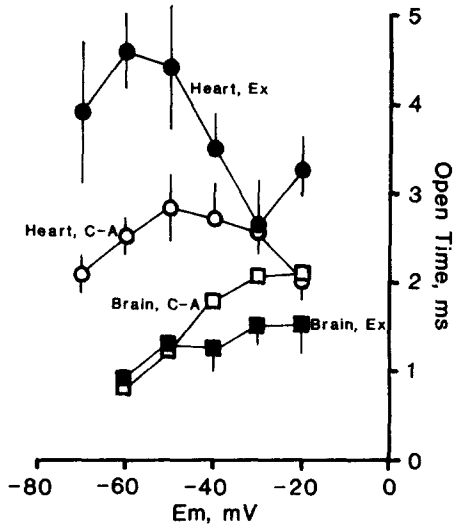

FIGURE 6. Voltage dependence of mean open times of neuronal and cardiac Na channels. Mean open times from different patches were averaged and the SE of the mean was calculated. SE bars were omitted when they were smaller than the symbol. Data were obtained in excised ventricular patches (both inside-out and outside-out, filled circles, $n = 8$), outside-out neuronal patches (filled squares, $n = 5$), cell-attached ventricular patches (open circles, $n = 10$), and cell-attached neuronal patches (open squares, $n = 4$). Cell-attached recordings were obtained from heart cells bathed in depolarizing solution (either KCl or KF). Brain cells would not tolerate low Ca^{2+} depolarizing solution, and absolute membrane potentials were estimated from the single-channel current-voltage relationship.

In ventricular myocytes bathed in low Ca KF-depolarizing solution we were able to record single-channel currents both before and after patch excision. Fig. 7 shows an example of such an experiment. In the cell-attached mode (Fig. 7 *A*) Na channel open time was brief (mean, 1.8 ms) and short bursts were occasionally observed. Within 5 min of patch excision into the inside-out mode (Fig. 7 *B*) both mean open time (6.7 ms) and burst duration increased markedly such that single-channel bursts sometimes extended over nearly the entire duration of the 140-ms test pulse. In this experiment average waiting time was slightly reduced and mean single-channel amplitude was not altered by patch excision. A comparison of average waiting times in other excised and cell-attached heart patches showed that patch excision shifted the voltage dependence of activation ~−10 mV, a result which is consistent with previous reports of a negative shift in the voltage dependence of activation in

excised patches (Fernandez et al., 1984; Kunze et al., 1985). Nonetheless, as shown in Fig. 6, shifting the voltage dependence of open time along the voltage axis cannot account for the observed differences between cell-attached and excised heart patches. Furthermore, the observation that bursting occurred in a patch exposed to KF-rich solution rules out the possibility that the effect depends on the interaction of Cs^+ with the inactivation gate (Oxford and Yeh, 1985).

Excision-induced bursting in heart channels might be an artifact of exposure of the intracellular membrane surface to an artificial environment. Alternatively, modulation of channel gating may be a physiologically relevant property of heart chan-

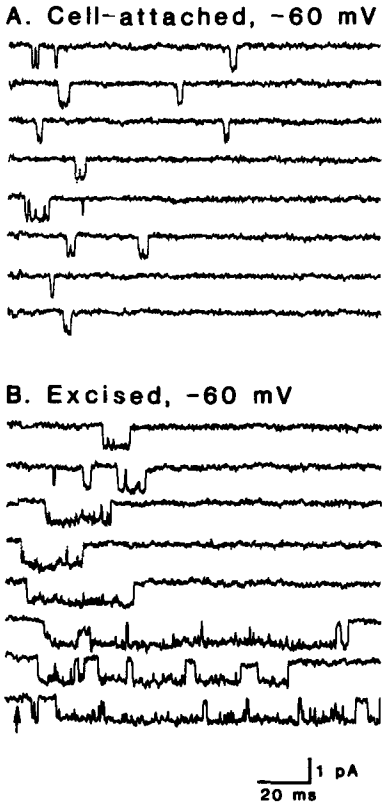

FIGURE 7. Single-channel currents in a ventricular myocyte before (*A*) and 5 min after (*B*) patch excision. The test pulse potential was −60 mV. Holding potential and prepulse potentials were −100 and −140, respectively; other recording details were as related in Fig. 1. The cell was bathed in KF solution, the pipette contained Tyrode's. Mean single-channel amplitude was 0.94 and 0.98 respectively, in *A* and *B*. Mean open time was 1.8 and 6.7 ms, respectively, in *A* and *B*. Mean waiting time was 15 and 12 ms, respectively, in *A* and *B*. Temperature, 10.0°C.

nels that is potentiated by cell-free recording conditions. As shown in Fig. 8, one of ten cell-attached patches exhibited bursting that resembled that found in excised patches. Fig. 8 *A* shows sequential traces obtained at a test potential of −60 mV from a holding potential of −100 mV. Long-lasting bursts were prominent in traces 2, 8, and 11. The histogram of open-time distribution from these and other records from the same patch was accurately described by the sum of two exponentials with time constants (and weighting factors) of 1.4 (0.8) and 6.4 (0.2). The short and long time constants of the open-time histogram closely match those obtained from other patches under cell-attached and excised patch conditions, respectively, which suggests a mixed population of modified and unmodified channels. Burst duration dis-

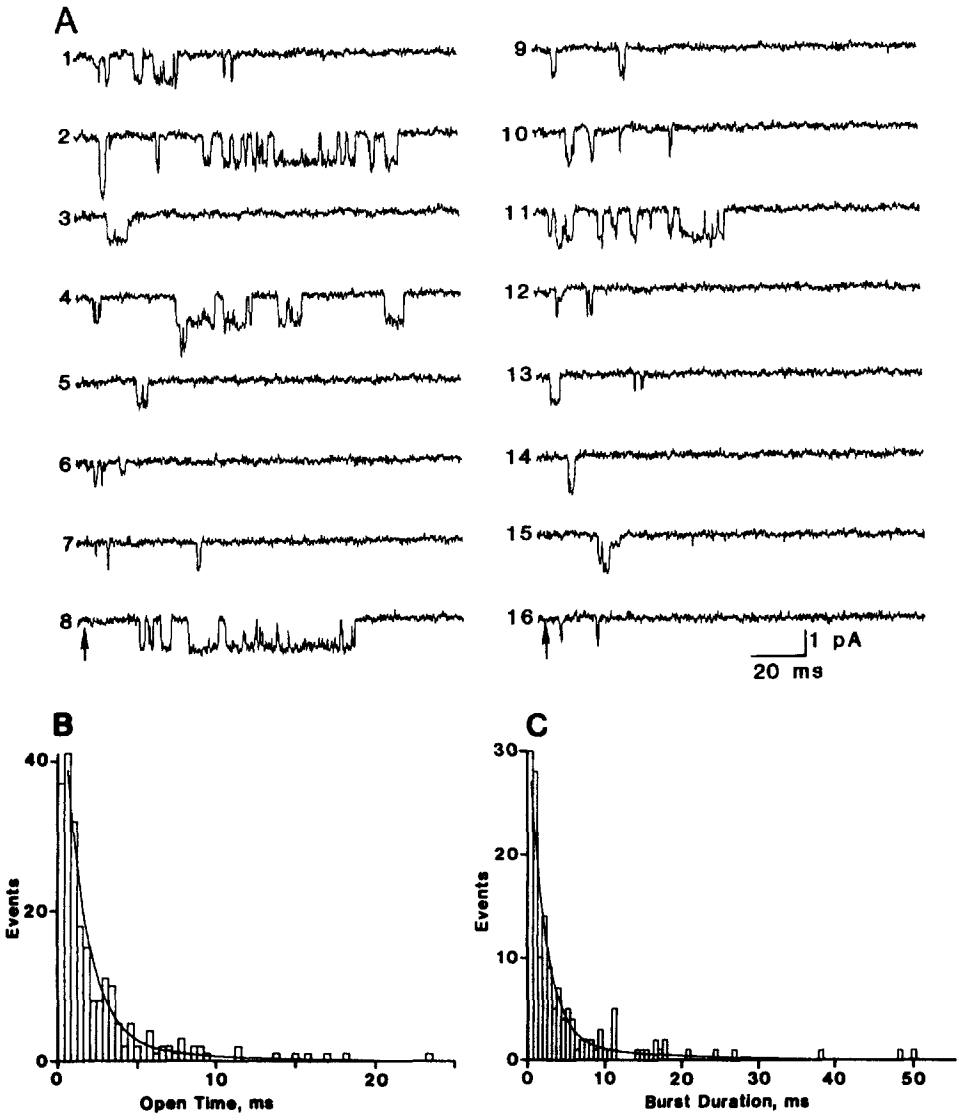

FIGURE 8. Burst activity in a cell-attached ventricular patch at test potential −60. Holding potential and prepulse potentials were −100 and −120 mV, respectively. The pipette contained Tyrode's solution; the bath solution was KCl-depolarizing. Sequential traces are illustrated, prominent bursting appears in traces 2, 8, and 11. The open-time histogram (*B*) was fit by sum of two exponentials with time constants (and weighting factors): 1.4 (0.8) and 6.4 (0.2). The maximum closed time in burst, 1.8 ms, was estimated (Colquhoun and Sakmann, 1985) from the closed-time histogram (not shown). Burst duration histogram (*C*) was fit by the sum of two exponentials with time constants (and weighting factors): 2.0 ms (0.73) and 12.9 ms (0.27). Temperature, 10.5°C.

tribution (Fig. 8 *C*) was accurately described by the sum of two exponentials with time constants (and weighting factors) of 2.0 (0.7) and 12.9 (0.3) ms, which closely match those obtained from the excised patch in Fig. 5 *B*, except that the probability of observing long bursts was lower. These results suggest that patch excision shifts gating toward a long burst, long mean open-time mode.

DISCUSSION

The first important observation in this study is that under identical conditions, gating of single cardiac Na channels is slower than gating of single neuronal Na channels. In excised patches heart channels had markedly longer open times, waiting times, and burst durations. The second important observation is that patch excision caused prolonged open time and bursting in heart but not in brain channels.

Our analysis of single brain Na channels shows that these channels follow a kinetic pattern similar to that proposed by Aldrich et al. (1983) for neuroblastoma Na channels. We saw no evidence of repetitive opening of single Na channels and inactivation of the ensemble average current could be described by a monoexponential decay. A slow phase of Na current inactivation has been reported to develop in cortical neurons from older rats (>6 d old; Huguenard et al., 1988) and in dorsal root ganglion cells (Kostyuk et al., 1981). In the latter case however, the slowly inactivating Na current was shown to be TTX-resistant, and thus it may arise from a different Na channel subtype. A similar TTX-insensitive, slowly inactivating current has been identified in adult rat nodose ganglion cells (Ikeda et al., 1986). In the experiments described here, Na channels were completely blocked by 1 μM TTX, and this rapidly inactivating Na channel appears to predominate in neonate cortical neurons. Evidence of TTX-insensitive and noninactivating channels was also obtained (see Fig. 1). Whether these channels are Na channel subtypes remains to be determined.

The bursting and long open times observed in excised heart patches suggests that Na channel inactivation is modified under cell-free conditions. The observation that similar behavior is sometimes observed in cell-attached patches suggests that inactivation in heart is modulated by some type of intracellular mechanism. Modulation of slowly-inactivating inward Na currents may be particularly important in cardiac muscle as a means of regulating the duration of the action potential.

Prolonged bursting has been described previously in cardiac muscle Na channels, but the frequency of occurrence of such events was usually <0.1% in channels recorded in the cell-attached mode (Patlak and Ortiz, 1985; Grant and Starmer, 1987; Clark and Giles, 1987) and in channels recorded in excised patches exposed on the intracellular surface to a predominantly CsCl-containing solution (Kohlhardt et al., 1987). The relatively frequent occurrence of bursting in our experiments with excised patches may be related to the use of an intracellular solution containing F as the main anion. Fluoride has been shown previously to slow the activation kinetics of K channels in squid axon in a reversible manner (Adams and Oxford, 1983, Kirsch et al., 1986) and to reversibly activate the muscarinic K channel in atrial myocytes by a GTP-binding protein mechanism (Kurachi and Nakajima, 1987). Whether similar mechanisms also operate on Na channels remains to be investigated. None-

theless, such modulation would have important physiological consequences since the depolarizing effects of maintained inward Na current could have a profound effect on cardiac rhythmicity.

This work was supported by American Heart Association grant 876197 to G. E. Kirsch, and by National Heart, Lung and Blood Institute grants Hl-25143 and HL-33662 to A. M. Brown.

Original version received 26 May 1988 and accepted version received 7 July 1988.

REFERENCES

Adams, D. J., and G. S. Oxford. 1983. Interaction of internal anions with potassium channels of the squid giant axon. *Biophysical Journal.* 82:429–448.

Aldrich, R. W., D. P. Corey, and C. F. Stevens. 1983. A reinterpretation of mammalian sodium channel gating based on single channel recording. *Nature.* 306:436–441.

Bean, B. P., C. J. Cohen, and R. W. Tsien. 1983. Lidocaine block of cardiac sodium channels. *Journal of General Physiology.* 81:613–642.

Brown, A. M., K. S. Lee, and T. Powell. 1981. Sodium current in single rat heart muscle cells. *Journal of Physiology.* 318:479–500.

Chiu, S. Y. 1977. Inactivation of sodium channels: second order kinetics in myelinated nerve. *Journal of Physiology.* 273:573–596.

Clark, R. B., and W. Giles. 1987. Sodium current in single cells from bullfrog atrium: voltage dependence and ion transfer properties. *Journal of Physiology.* 391:235–265.

Colquhoun, D., and B. Sakmann. 1985. Fast events in single-channel currents activated by acetylcholine and its analogues at the frog muscle end-plate. *Journal of Physiology.* 369:501–557.

Cruz, L. J., W. R. Gray, B. M. Olivera, R. D. Zeikus, L. Kerr, D. Yoshikami, and E. Moczydlowski. 1985. *Conus geographicus* toxins that discriminate between neuronal and muscle sodium channels. *Journal of Biological Chemistry.* 260:9280–9288.

Davis, L. D., and J. V. Temte. 1969. Electrophysiological actions of lidocaine on canine ventricular muscle and Purkinje fibers. *Circulation Research.* 24:639–655.

Dudel, J. K., R. Peper, R. Rudel, and W. Trautwein. 1967. The effect of tetrodotoxin on the membrane current in cardiac muscle (Purkinje fibers). *Pflügers Archiv.* 295:213–226.

Fernandez, J. M., A. P. Fox, and S. Krasne. 1984. Membrane patches and whole-cell membranes: a comparison of electrical properties in rat clonal pituitary (GH_3) cells. *Journal of Physiology.* 356:565–585.

Follmer, C. H., R. E. Ten Eick, and J. Z. Yeh. 1987. Sodium current kinetics in cat atrial myocytes. *Journal of Physiology.* 384:169–197.

Grant, A. O., and C. F. Starmer. 1987. Mechanisms of closure of cardiac sodium channels in rabbit ventricular myocytes: single-channel analysis. *Circulation Research.* 60:897–913.

Hamill, O. P., A. Marty, B. Sakmann, and F. J. Sigworth. 1981. Improved patch-clamp techniques for high-resolution current recording from cells and cell-free membrane patches. *Pflügers Archiv.* 391:85–100.

Huguenard, J. R., O. P. Hamill, and D. A. Prince. 1988. Developmental changes in Na conductances in rat neonatal neurons: appearance of a slowly inactivating component. *Journal of Neurophysiology.* 59:778–795.

Ikeda, S. R., G. G. Schofield, and F. F. Weight. 1986. Na and Ca^{2+} currents of acutely isolated adult rat nodose ganglion cells. *Journal of Neurophysiology.* 55:527–539.

Kirsch, G. E., and A. M. Brown. 1988. Single channels in rat heart and rat brain have different kinetic properties. *Biophysical Journal.* 53:227. (Abstr.)

Kirsch, G. E., J. Z. Yeh, and G. S. Oxford. 1986. Modulation of aminopyridine block of potassium currents in squid axon. *Biophysical Journal.* 50:637–644.

Kohlhardt, M., U. Frobe, and J. W. Herzig. 1987. Properties of normal and non-inactivating single cardiac Na channels. *Proceedings of the Royal Society Series B.* 232:71–93.

Kostyuk, P. G., N. S. Veselovsky, and A. Y. Tsyndrenko. 1981. Ionic currents in the somatic membrane of rat dorsal root ganglion neurons-I sodium currents. *Neuroscience.* 6:2423–2430.

Kunze, D. L., A. E. Lacerda, D. L. Wilson, and A. M. Brown. 1985. Cardiac Na currents and the inactivating, reopening, and waiting properties of single cardiac Na channels. *Journal of General Physiology.* 86:691–719.

Kurachi, Y., and T. Nakajima. 1987. Intracellular fluoride activation of muscarinic K channel in atrial cell membrane. *Circulation.* 76:105 (Abstr.)

Lux, H. D., and A. M. Brown. 1984. Patch and whole cell calcium currents recorded simultaneously in snail neurons. *Journal of General Physiology.* 83:727–750.

Narahashi, T. 1974. Chemicals as tools in the study of excitable membranes. *Physiological Review.* 54:813–889.

Oxford, G. S., and J. Z. Yeh. 1985. Interactions of monovalent cations with sodium channels in squid axon. I. Modification of physiological inactivation gating. *Journal of General Physiology.* 85:583–602.

Patlak, J., and R. Horn. 1982. Effect of *N*-bromoacetamide on single sodium channel currents in excised membrane patches. *Journal of General Physiology.* 79:333–351.

Patlak, J. B., and M. Ortiz. 1985. Slow currents through single sodium channels of adult rat heart. *Journal of General Physiology.* 86:89–104.

Yatani, A., and A. M. Brown. 1985. The calcium channel blocker nitrendipine blocks sodium channels in neonatal rat cardiac myocytes. *Circulation Research.* 57:868–875.